Int. J. Heat Mass Transfer. Vol. 34, No. 10, pp. 2581–2592, 1991
Printed in Great Britain

0017–9310/91 $3.00+0.00

Unsteady thermal entrance heat transfer in laminar flow with a periodic variation of inlet temperature

WEIGONG LI and SADIK KAKAC
Department of Mechanical Engineering, University of Miami, Coral Gables, FL 33124, U.S.A.

(*Received 5 February* 1990 *and in final form* 26 *November* 1990)

Abstract—A theoretical study of laminar forced convection in the thermal entrance region of a rectangular duct, subjected to a sinusoidally varying inlet temperature, is presented. Several boundary conditions that account for uniform wall heat flux and/or external convections with or without wall thermal capacitance effects are considered. Analytical expressions for these problems are obtained through extending the generalized integral transform technique. The centerline temperature amplitudes are determined as a function of Biot number, fluid-to-wall thermal capacitance ratio and dimensionless inlet frequency of inlet heat input oscillations. The effects of these variables on the solution are discussed. The eigenvalues and corresponding coefficients are given in tabular forms.

INTRODUCTION

STEADY and unsteady duct flows with unsteady forced convection are of great interest in connection with the increasingly greater use of automatic control devices for the accurate control of fluid flow in heat exchange equipment. Accurate prediction of the transient response of heat exchange equipment is highly important, not only to provide for an effective control system, but also important for understanding of undesirable effects such as reduced thermal performance and severe thermal stresses which can be produced, with eventual mechanical failure. Thus, the thermal response of unsteady temperature subjected to a periodic variation of inlet temperature is of great interest in engineering applications and also important for effective thermal equipment control systems, such as heat exchangers and their control.

Solutions to this problem lead to the solution of complex eigenvalue problems, which are not of the conventional Sturm–Liouville type; the eigenvalues and corresponding eigenfunctions are complex numbers and complex valued functions, respectively. The main task in the analysis of such problems has been the difficulty in finding solutions of the resulting complex eigenvalue problem.

Sparrow and De Farias [1] presented an analysis of periodic forced convection with slug flow in a parallel plate channel with sinusoidally varying inlet temperature and time- and space-dependent wall temperature. The wall temperature was dynamically determined by a balance of the heat transfer rate and the energy storage. Numerical evaluation of the analytical results provided the time and space dependence of the wall and bulk temperatures and the Nusselt number. Their work appears to be the first analysis of this type of problem. An exact solution to the transient energy equation for laminar slug flow in a parallel plate channel with a sinusoidal variation of inlet temperature was obtained in ref. [2]. A general solution to the transient energy equation under constant wall temperature or zero heat flux boundary conditions for the decay of inlet temperature distributions of incompressible transient forced convection between parallel plates was obtained in ref. [3]. Cotta and Ozisik [4] solved the slug flow problem considered in refs. [1, 2], for both circular tubes and parallel plate channels, by developing an approach for complex transcendental equations and providing accurate results for the related eigenvalues. Later, Cotta *et al.* [5] extended their previous study to laminar forced convection under the constant wall temperature condition.

Kakac *et al.* [6, 7] designed and built an experimental set-up and carried out some experimental research. Recently, they compared the experimental findings with the theoretical studies of the temperature amplitude at the centerline of the rectangular duct [8, 9]. The comparison showed that the theoretical analysis is in good agreement with the experimental investigation.

In the present work, the unsteady laminar forced convection in the thermal entrance region of a parallel plate channel is considered. The problems for other duct geometries could be solved by the same method and procedure.

The inlet temperature is assumed to vary periodically with time. The thermal response of the system to these variations is to be determined after the initial transients die out. In practical applications, the inlet temperature of a heat exchanger may vary as a function of time. A general time-dependent inlet condition can be expanded in terms of sine and cosine function by use of Fourier series. Therefore, authors believe

NOMENCLATURE

a^* fluid-to-wall thermal capacitance ratio, $\rho C_p d/(\rho_w C_w L)$
a_n constant, defined by equation (17)
a_{nk} element of matrix **A**, defined by equation (9b)
A dimensionless temperature amplitude function
A $N \times N$ matrix, defined by equation (27)
A_{nk} coefficient, defined by equation (25)
Bi modified Biot number, $h_e d/k$ [dimensionless]
c_n coefficient, defined by equation (41)
C_w equivalent wall specific heat [kJ kg^{-1} K^{-1}]
C_p specific heat of the fluid at constant pressure [kJ kg^{-1} K^{-1}]
d half distance between parallel plates [m]
D_e equivalent diameter of parallel plate channel, $4d$ [m]
e_n constant, defined by equation (18)
f_n coefficient, defined by equation (24b)
F_n coefficient, defined by equation (50)
f^+ coefficient vector, defined by equation (26b)
g_n coefficient, defined by equation (45)
G_n coefficient, defined by equation (46)
h convective heat transfer coefficient outside the wall [W m^{-2} K^{-1}]
h_e equivalent heat transfer coefficient between inner wall and ambient fluid at temperature T_∞, $(1/h + L/k_w)^{-1}$ [W m^{-2} K^{-1}]
i imaginary number, $\sqrt{-1}$
Im imaginary part of the complex value in equations (52)
k fluid thermal conductivity [W m^{-1} K^{-1}]
L thickness of the wall
N number of terms in series
N_n norm of the eigenproblem defined by equation (19)
Nu Nusselt number, hd/k
Pr Prandtl number, v/α [dimensionless]
q wall heat flux, $q_w d/(k\Delta T_c)$ [dimensionless]
q_w wall heat flux [W m^{-2}]
Re Reynolds number, $U_m D_e/v$ [dimensionless]
Re real part of the complex value in equations (52)
t time variable [s]
T temperature [K]
$\Delta T(y)$ inlet temperature amplitude profile
T_∞ ambient temperature around the experimental set-up [K]
$u(y)$ velocity profile across the test section [m s^{-1}]
$U(\eta)$ dimensionless velocity profile
U_m mean velocity [m s^{-1}]
v_n^+ nth eigenvector of problem (39)
x axial coordinate [m]
y normal coordinate [m]
Y_n eigenfunction corresponding to the nth eigenvalue, defined by equation (5).

Greek symbols
α fluid thermal diffusivity, $k/\rho C_p$ [m s^{-2}]
β inlet frequency [Hz]
δ_{nk} δ function: for $n = k$, $\delta_{nk} = 1$; for $n \neq k$, $\delta_{nk} = 0$
η normal coordinate, y/d [dimensionless]
$\theta(\xi, \eta, \tau)$ dimensionless temperature
$\tilde{\theta}(\xi, \eta)$ quasi-steady dimensionless temperature, defined by equation (3)
$\tilde{\theta}_n(\xi, \eta)$ integral transfer, defined by equation (23)
θ^+ nth eigenvector for equation (9a)
$\Delta\theta(\eta)$ inlet temperature amplitude profile, $\Delta T(y)/\Delta T_c$ [dimensionless]
λ_n nth eigenvalue
μ_n eigenvalues of equation (9a)
ξ axial coordinate, $(x/D_e)(D_e/d)^2/(Re\,Pr)$ [dimensionless]
ρ fluid density [kg m^{-3}]
ρ_w equivalent density of the wall [kg m^{-3}]
τ time, $\alpha t/d^2$ [dimensionless]
ϕ phase lag
Ω inlet frequency, $2\pi\beta d^2/\alpha$ [dimensionless].

Superscript
1 lowest order solution.

Subscripts
c centerline value
w value at the wall.

that the results of sinusoidal variation of inlet temperature is very basic for further research of the unsteady forced convection under the general time-dependent inlet condition.

The theoretical analysis is extended to more general boundary conditions of the problem given in ref. [8]. Analytical results are discussed for various parameters, such as modified Biot number and fluid-to-wall thermal capacitance ratio, which are difficult to perform in the experiments. The eigenvalues and corresponding coefficients are also listed in the tables, which could be used to predict the temperature distribution and to evaluate the unsteady performance inside the channel of a heat exchanger.

PROBLEM FORMULATION

Let us consider unsteady forced convection with fully developed laminar flow through parallel plates whose walls are separated by a distance of $2d$, as shown in Fig. 1.

Assuming that the fluid flows through the duct with negligible viscous dissipation, negligible axial diffusion and constant fluid thermophysical properties, the energy equation governing the diffusion in the y-direction and the convection in the x-direction for the thermal entrance region can be written as

$$\frac{\partial T}{\partial t}+u(y)\frac{\partial T}{\partial x}=\alpha\frac{\partial^2 T}{\partial y^2},$$

$$\text{for } x>0,\ 0<y<d,\ t>0. \quad (1)$$

Let us consider the inlet condition for this problem to be the real part of the following periodic condition:

$$T(0,y,t)=T_\infty+\Delta T(y)\,e^{i\beta t},\quad \text{for } 0<y<d,\ t>0. \quad (2)$$

In addition to the inlet condition, equation (1) should satisfy the symmetry condition at the centerline of the duct

$$\frac{\partial T}{\partial y}=0,\quad \text{at } y=0,\ \text{for } x>d,\ t>0. \quad (3)$$

At the outside of the walls, three kinds of boundary condition could be specified:

(1) Constant heat flux across the walls

$$-k\frac{\partial T}{\partial y}=q_w,\quad \text{at } y=d,\ \text{for } x>0,\ t>0. \quad (4a)$$

(2) Neglecting the effects of wall thickness and wall thermal capacitance, only considering the external convective heat transfer

$$\left[h(T-T_\infty)+k\frac{\partial T}{\partial y}\right]=0,$$

$$\text{at } y=d,\ \text{for } x>0,\ t>0. \quad (4b)$$

(3) Accounting for both external convection and wall thermal capacitance

$$h_e(T-T_\infty)+k\frac{\partial T}{\partial y}+(\rho C)_w L\frac{\partial T}{\partial t}=0,$$

$$\text{at } y=d,\ \text{for } x>0,\ t>0. \quad (4c)$$

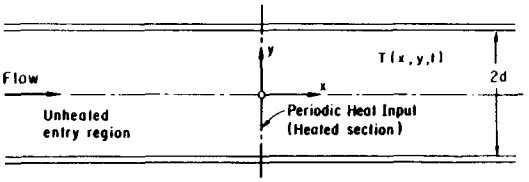

FIG. 1. The geometry of the theoretical analysis.

Here the initial condition is not necessary, since only the periodic solution is of interest.

With the introduction of the following dimensionless parameters:

$$\eta=y/d,\ \xi=(x/D_e)(D_e/d)^2/(Re\,Pr),$$

$$\tau=\alpha t/d^2,\ \theta=(T-T_\infty)/\Delta T_c$$

$$\Omega=\beta d^2/\alpha,\ q=q_w d/(k\Delta T_c),\ Nu=hd/k,$$

$$Bi=h_e d/k,\ a^*=(\rho C_p)_f d/\rho_w C_w L \quad (5)$$

and

$$U(\eta)=u(y)/U_m,\ \Delta\theta(\eta)=\Delta T(y)/\Delta T_c. \quad (6)$$

Equations (1)–(4) can now be rewritten in dimensionless form as:

governing equation

$$\frac{\partial\theta}{\partial\tau}+U(\eta)\frac{\partial\theta}{\partial\xi}=\frac{\partial^2\theta}{\partial\eta^2},$$

$$\text{for } 0<\eta<1,\ \xi>0,\ \tau>0 \quad (7)$$

inlet condition

$$\theta(0,\eta,\tau)=\Delta\theta(\eta)\,e^{i\Omega\tau},\quad \text{for } \tau>0 \quad (8)$$

symmetry condition

$$\frac{\partial\theta}{\partial\eta}=0,\quad \text{at } \eta=0,\ \text{for } \xi>0,\ \tau>0 \quad (9)$$

constant wall heat flux condition

$$\frac{\partial\theta}{\partial\eta}=-q,\quad \text{at } \eta=0,\ \text{for } \xi>0,\ \tau>0 \quad (10a)$$

convective heat transfer condition without considering the wall thermal capacitance

$$Nu\,\theta+\frac{\partial\theta}{\partial\eta}=0,\quad \text{at } \eta=1,\ \text{for } \xi>0,\tau>0$$

(10b)

convective heat transfer condition considering the wall thermal capacitance

$$Bi\,\theta+\frac{\partial\theta}{\partial\eta}+\frac{1}{a^*}\frac{\partial\theta}{\partial\tau}=0,$$

$$\text{at } \eta=1,\ \text{for } \xi>0,\ \tau>0. \quad (10c)$$

If Nu goes to infinity, equation (10b) gives a constant wall temperature boundary condition; if Nu goes to zero, equation (10b) becomes an insulated boundary condition. If a^* goes to infinity, then the wall capacitance effects become negligible in equation (10c), the modified Biot number (Bi) becomes the Nusselt number (Nu). Thus, equation (10c) approaches to equation (10b).

The solution to the unsteady state energy equation (7) with inlet condition (8) under the three different boundary conditions (10a)–(10c) together with (9) are presented in the following sections.

Case I

In this case we consider the governing equation under the constant wall heat flux boundary condition.

For this boundary condition, the governing equation, inlet condition and boundary conditions are as follows:

$$\frac{\partial\theta}{\partial\tau}+U(\eta)\frac{\partial\theta}{\partial\xi}=\frac{\partial^2\theta}{\partial\eta^2},$$

$$\text{for } 0<\eta<1,\ \xi>0,\ \tau>0 \quad (11a)$$

$$\theta(0,\eta,\tau)=\Delta\theta(\eta)\,e^{i\Omega\tau},\quad \text{for } 0<\eta<1,\ \tau>0 \quad (11b)$$

$$\frac{\partial\theta}{\partial\eta}=0,\quad \text{at } \eta=0,\ \text{for } \xi>0,\ \tau>0 \quad (11c)$$

$$\frac{\partial\theta}{\partial\eta}=-q,\quad \text{at } \eta=1,\ \text{for } \xi>0,\ \tau>0. \quad (11d)$$

The following Sturm–Liouville problem can be determined by the numerical method, such as, the 'sign-count' method [10], for a parabolic velocity profile $U(y)$

$$\frac{d^2Y_n}{dy^2}+\lambda_n^2U(y)Y_n=0,\quad \text{for } 0<y<1 \quad (12a)$$

$$\frac{dY_n}{dy}=0,\quad y=0 \quad (12b)$$

$$\frac{dY_n}{dy}=0,\quad y=1. \quad (12c)$$

We separate the dimensionless temperature distribution into two parts as $\theta_1(\xi,\eta)$ and $\theta_2(\xi,\eta,\tau)$

$$\theta(\xi,\eta,\tau)=\theta_1(\xi,\eta)+\theta_2(\xi,\eta,\tau) \quad (13)$$

in which $\theta_1(\xi,\eta)$ and $\theta_2(\xi,\eta,\tau)$ satisfy the following differential equations and inlet boundary conditions:

$$U(\eta)\frac{\partial\theta_1}{\partial\xi}=\frac{\partial^2\theta_1}{\partial\eta^2},\quad \text{for } 0<\eta<1,\ \xi>0 \quad (14a)$$

$$\theta_1(0,\eta)=0,\quad \text{for } 0<\eta<1 \quad (14b)$$

$$\frac{\partial\theta_1}{\partial\eta}=0,\quad \text{at } \eta=0,\quad \text{for } \xi>0 \quad (14c)$$

$$\frac{\partial\theta_1}{\partial\eta}=-q,\quad \text{at } \eta=1,\quad \text{for } \xi>0 \quad (14d)$$

and

$$U(\eta)\frac{\partial\theta_2}{\partial\tau}+\frac{\partial\theta_2}{\partial\xi}=\frac{\partial^2\theta_2}{\partial\eta^2},$$

$$\text{for } 0<\eta<1,\ \xi>0,\ \tau>0 \quad (15a)$$

$$\theta_2(0,\eta,\tau)=\Delta\theta(\eta)\,e^{i\Omega\tau},$$

$$\text{for } 0<\eta<1,\ \tau>0 \quad (15b)$$

$$\frac{\partial\theta_2}{\partial\eta}=0,\quad \text{at } \eta=0,\ \text{for } \xi>0,\ \tau>0 \quad (15c)$$

$$\frac{\partial\theta_2}{\partial\eta}=0,\quad \text{at } \eta=1,\ \text{for } \xi>0,\ \tau>0. \quad (15d)$$

(1) *Solution for* $\theta_1(\xi,\eta)$. The solution of $\theta_1(\xi,\eta)$ is obtained by the method of separation of variables and is given by [11]

$$\theta_1(\xi,\eta)=-\frac{q}{2}\eta^2-\frac{q}{2}\sum_{n=0}^{N}\frac{a_n}{N_n}\exp(-\lambda_n^2\xi)Y_n(\eta)$$
$$-q\sum_{n=0}^{N}\frac{e_n}{N_n\lambda_n^2}[1-\exp(-\lambda_n^2\xi)]Y_n(\eta) \quad (16)$$

where

$$a_n=\int_0^1U(\eta)\eta^2Y_n(\eta)\,d\eta \quad (17)$$

$$e_n=\int_0^1Y_n(\eta)\,d\eta \quad (18)$$

$$N_n=\int_0^1U(\eta)\,Y_n^2(\eta)\,d\eta. \quad (19)$$

(2) *Solution for* $\theta_2(\xi,\eta,\tau)$. Since the boundary conditions for $\theta_2(\xi,\eta,\tau)$ are homogeneous, introducing

$$\theta_2(\xi,\eta,\tau)=e^{i\Omega\tau}\,\bar\theta(\xi,\eta) \quad (20)$$

and substituting equation (20) into equation (15), we obtain the following equations:

$$U(\eta)\frac{\partial^2\bar\theta}{\partial\eta^2}-\frac{\partial\bar\theta}{\partial\xi}-i\Omega\bar\theta=0,$$

$$\text{for } 0<\eta<1,\ \xi>0 \quad (21a)$$

$$\bar\theta(0,\eta)=\Delta\theta(\eta),\quad \text{for } 0<\eta<1 \quad (21b)$$

$$\frac{\partial\bar\theta}{\partial\eta}=0,\quad \text{at } \eta=0,\ \text{for } \xi>0 \quad (21c)$$

$$\frac{\partial\bar\theta}{\partial\eta}=0,\quad \text{at } \eta=1,\ \text{for } \xi>0. \quad (21d)$$

By the use of the eigenvalues and eigenfunctions determined by system (12), the following integral transform pairs are defined:

$$\bar\theta(\xi,\eta)=\sum_{n=0}^{N}\frac{1}{\sqrt{N_n}}\tilde\theta_n(\xi)Y_n(\eta) \quad (22)$$

and

$$\tilde\theta_n(\xi)=\int_0^1\frac{1}{\sqrt{N_n}}U(\eta)\,Y_n(\eta)\bar\theta(\xi,\eta)\,d\eta. \quad (23)$$

Equation (21a) and inlet condition, equation (21b), could be transformed to problem (24) by multiplying both sides of the equations by $Y_k(\eta)$, and integrating them

$$\frac{d\tilde\theta_k}{d\xi}+\lambda_k^2\tilde\theta_k+i\Omega\sum_{n=0}^{N}\tilde\theta_nA_{nk}=0 \quad (24a)$$

$$\tilde\theta_k(0)=\int_0^1\frac{1}{\sqrt{N_k}}U(\eta)\Delta\theta(\eta)\,Y_k\,d\eta=f_k \quad (24b)$$

where

$$A_{nk} = A_{kn} = \int_0^1 \frac{1}{\sqrt{(N_n N_k)}} Y_n Y_k \, d\eta. \quad (25)$$

Taking a very large (but finite) N in the summation to satisfy any accuracy criterion, $\theta^+(\xi)$ and f^+ can be defined as

$$\theta^+(\xi) = (\bar{\theta}_0, \bar{\theta}_1, \ldots, \bar{\theta}_N) \quad (26a)$$

$$f^+ = (f_0, f_1, \ldots, f_N) \quad (26b)$$

and an $(N+1) \times (N+1)$ matrix $\mathbf{A}$ by

$$a_{ij} = (\delta_{ij}\lambda_i^2 + i\Omega A_{ij}) \quad (i, j = 0, 1, 2, \ldots, N) \quad (26c)$$

then, equations (24) can be rewritten as

$$\frac{d\theta^+}{d\xi} + \mathbf{A}\theta^+ = 0 \quad (27a)$$

$$\theta^+(0) = f^+. \quad (27b)$$

Usually, it is very difficult to get the analytical solution for θ^+, however, the numerical solution may easily be found. After solving for θ^+, and returning to equations (22) and (20), the solutions for $\theta_2(\xi, \eta, \tau)$ and $\theta(\xi, \eta, \tau)$ can be determined. The details of obtaining the solution are given in the next section.

Case II

For the convective boundary condition without considering the effect of wall thermal capacitance, the governing equation, inlet condition and boundary conditions are respectively

$$\frac{\partial\theta}{\partial\tau} + U(\eta)\frac{\partial\theta}{\partial\xi} = \frac{\partial^2\theta}{\partial\eta^2}, \quad \text{for } 0 < \eta < 1, \ \xi > 0, \ \tau > 0 \quad (28a)$$

$$\theta(0, \eta, \tau) = \Delta\theta(\eta)\, e^{i\Omega\tau}, \quad \text{for } 0 < \eta < 1, \ \tau > 0 \quad (28b)$$

$$\frac{\partial\theta}{\partial\eta} = 0, \quad \text{at } \eta = 0, \text{ for } \xi > 0, \ \tau > 0 \quad (28c)$$

$$\left(Nu\,\theta + \frac{\partial\theta}{\partial\eta}\right) = 0, \quad \text{at } \eta = 1, \text{ for } \xi > 0, \ \tau > 0. \quad (28d)$$

The related eigenvalue problem is specified by the following:

$$\frac{d^2 Y_n}{dy^2} + \lambda_n^2 U(y) Y_n = 0 \quad (29a)$$

$$\frac{dY_n}{dy} = 0, \quad y = 0 \quad (29b)$$

$$\left(Bi\, Y_n + \frac{dY_n}{dy}\right) = 0, \quad y = 1. \quad (29c)$$

For this condition, it is not necessary to separate the dimensionless temperature $\theta(\xi, \eta, \tau)$ as the superposition of two solutions as we did before, because of the homogeneous boundary conditions.

Introducing the same definitions and assumptions for Case I, we can find the same formulations for $\theta(\xi, \eta, \tau)$, as $\theta_2(\xi, \eta, \tau)$ as in Case I.

Assuming

$$\theta(\xi, \eta, \tau) = e^{i\Omega\tau}\bar{\theta}(\xi, \eta) \quad (30)$$

the problem for $\theta(\xi, \eta, \tau)$ is then changed to a problem for $\bar{\theta}(\xi, \eta)$, as

$$U(\eta)\frac{\partial^2\theta}{\partial\eta^2} - \frac{\partial\bar{\theta}}{\partial\xi} - i\Omega\bar{\theta} = 0, \quad \text{for } 0 < \eta < 1, \ \xi > 0 \quad (31a)$$

$$\bar{\theta}(0, \eta) = \Delta\theta(\eta), \quad \text{for } 0 < \eta < 1 \quad (31b)$$

$$\frac{\partial\bar{\theta}}{\partial\eta} = 0, \quad \text{at } \eta = 0, \text{ for } \xi > 0 \quad (31c)$$

$$Nu\,\bar{\theta} + \frac{\partial\bar{\theta}}{\partial\eta} = 0, \quad \text{at } \eta = 1, \text{ for } \xi > 0. \quad (31d)$$

By using the eigenfunctions determined by equations (29), defining the integral transform pairs as in Case I, equations (22) and (23), transforming equations (31) by multiplying both sides of the equations by $Y_k(\eta)$, and then integrating them, by the same procedures as before, the same differential equations for $\bar{\theta}_n(\xi)$ and vector–matrix expression, as in Case I, equations (26) could be obtained.

Note that the eigenvalues and eigenfunction in this case are different from those in Case I.

Case III

For the convective boundary condition which considers the effect of wall thermal capacitance, the governing equation, inlet and boundary conditions are rewritten as follows:

$$\frac{\partial\theta}{\partial\tau} + U(\eta)\frac{\partial\theta}{\partial\xi} = \frac{\partial^2\theta}{\partial\eta^2}, \quad \text{for } 0 < \eta < 1, \ \xi > 0, \ \tau > 0 \quad (32a)$$

$$\theta(0, \eta, \tau) = \Delta\theta(\eta)\, e^{i\Omega\tau}, \quad \text{for } 0 < \eta < 0, \ \tau > 0 \quad (32b)$$

$$\frac{\partial\theta}{\partial\eta} = 0, \quad \text{at } \eta = 0, \text{ for } \xi > 0, \ \tau > 0 \quad (32c)$$

$$Bi\,\theta + \frac{\partial\theta}{\partial\eta} + \frac{1}{a^*}\frac{\partial\theta}{\partial\tau} = 0, \quad \text{at } \eta = 1, \text{ for } \xi > 0, \ \tau > 0. \quad (32d)$$

The logic of solving this problem is a little different from the previous two cases. In this case, the periodic solution, such as

$$\theta(\xi, \eta, \tau) = e^{i\Omega\tau}\bar{\theta}(\xi, \eta) \quad (33)$$

is directly assumed for the decay of the inlet condition because of the homogeneous boundary condition. Substitution of equation (33) into equations (32) results in the following problem for $\bar{\theta}(\xi, \eta)$:

$$\frac{\partial^2\bar{\theta}}{\partial\eta^2} - U(\eta)\frac{\partial\bar{\theta}}{\partial\xi} - i\Omega\bar{\theta} = 0, \quad \text{for } 0 < \eta < 1, \ \xi > 0 \quad (34a)$$

$$\bar{\theta}(0,\eta)=\Delta\theta(\eta), \quad \text{for } 0<\eta<1 \tag{34b}$$

$$\frac{\partial\bar{\theta}}{\partial\eta}=0, \quad \text{at } \eta=0, \text{ for } \xi>0 \tag{34c}$$

$$Bi\,\bar{\theta}+\frac{\partial\bar{\theta}}{\partial\eta}=-\frac{i\Omega}{a^*}\bar{\theta}, \quad \text{at } \eta=1, \text{ for } \xi>0. \tag{34d}$$

First, we consider the homogeneous boundary condition, i.e. a^* approaches infinity. The corresponding eigenproblem is the same as that of Case II

$$\frac{d^2Y_n}{d\eta^2}+\lambda_n^2U(y)Y_n=0, \quad \text{for } 0<\eta<1 \tag{35a}$$

$$\frac{dY_n}{d\eta}=0, \quad \eta=0 \tag{35b}$$

$$Bi\,Y_n+\frac{dY_n}{d\eta}=0, \quad \eta=1. \tag{35c}$$

Introducing the integral-transform pairs for the function $\bar{\theta}(\xi,\eta)$, as defined in equations (22) and (23), and performing the same operation as in Case I, the following formulation is obtained:

$$\frac{d\tilde{\theta}_k}{d\xi}+\lambda_k^2\tilde{\theta}_k=\frac{1}{\sqrt{N_k}}\left[Y_k(1)\frac{\partial\bar{\theta}(\xi,1)}{\partial\eta}-\bar{\theta}(\xi,1)\frac{dY_k(1)}{d\eta}\right]-i\Omega\sum_{n=0}^{N}\times\frac{1}{\sqrt{N_n}}\tilde{\theta}_n(\xi)Y_n(\eta).$$

From manipulation of the boundary conditions, equations (34d) and (35c), the following is obtained:

$$\frac{1}{\sqrt{N_k}}\left[Y_k(1)\frac{\partial\bar{\theta}(\xi,1)}{\partial\eta}-\bar{\theta}(\xi,1)\frac{dY_k(1)}{d\eta}\right]=-\frac{i\Omega}{a^*}\bar{\theta}(\xi,1)\frac{Y_k(1)}{\sqrt{N_k}}$$

or, from the inversion formula, equation (22), one can obtain

$$\frac{i\Omega}{a^*}\bar{\theta}(\xi,1)\frac{Y_k(1)}{\sqrt{N_k}}=\frac{i\Omega}{a^*}\sum_{n=1}^{\infty}\frac{1}{\sqrt{(N_nN_k)}}Y_n(1)\,Y_k(1)\tilde{\theta}_n(\xi).$$

Equation (34a) and inlet condition (34b) could be transformed as

$$\frac{d\tilde{\theta}_k}{d\xi}+\lambda_k^2\tilde{\theta}_k+i\Omega\sum_{n=1}^{\infty}\tilde{\theta}_nA_{nk}=0 \tag{36a}$$

$$\tilde{\theta}_k(0)=\int_0^1\frac{1}{\sqrt{N_k}}U(\eta)\Delta\theta(\eta)Y_k\,d\eta=f_k \tag{36b}$$

where

$$A_{nk}=A_{kn}=\frac{1}{\sqrt{(N_nN_k)}}\left[\frac{Y_n(1)Y_k(1)}{a^*}+\int_0^1Y_nY_k\,d\eta\right] \tag{37}$$

which is different from the two previous cases. The same vector–matrix form as equations (27) could be worked out.

COMPLETE AND LOWEST ORDER SOLUTION

Complete solution

For different cases, the same formulation of the differential equation, as equations (27), is obtained

$$\frac{d\theta^+}{d\xi}+\mathbf{A}\theta^+=0 \tag{38a}$$

$$\theta^+(0)=f^+ \tag{38b}$$

where θ^+, f^+ and $\mathbf{A}$ are defined in equations (26). We can choose a sufficiently large N to satisfy any desired accuracy. The numerical study of truncating a different number of series terms has been carried out. It is shown that the convergent criterion of calculating the dimensionless amplitudes is smaller than 5×10^{-4} when $N>25$. Once the related eigenvalue problem of the $N\times N$ matrix $\mathbf{A}$, as defined by equation (26c)

$$(\mathbf{A}-\mu_n\mathbf{I})v_n^+=0 \tag{39}$$

is solved, the eigenvalues μ_n and eigenvectors v_n^+ $[v_{1n},v_{2n},\ldots,v_{Nn}]$, $(n=1,2,\ldots,N)$, can be determined.

The solution could be constructed from the linear combination of independent solutions

$$\tilde{\theta}_k(\xi)=\sum_{n=1}^{N}c_nv_{kn}\,e^{-\mu_n\xi}, \quad (k=1,2,\ldots,N) \tag{40}$$

where v_{kn} is the kth component of the nth eigenvector. By substituting the inlet condition equation (24b), the coefficients c_n can be determined from the following linear algebraic equations:

$$\sum_{n=1}^{N}c_nv_{kn}^+=f_k, \quad (k=1,2,\ldots,N). \tag{41}$$

The inversion formula equation (22) is then employed to provide the complete solution for $\bar{\theta}(\xi,\eta)$

$$\bar{\theta}(\xi,\eta)=\sum_{n=1}^{N}\sum_{k=1}^{N}\frac{1}{\sqrt{N_n}}c_kv_{nk}^+\,e^{-\mu_k\xi}\,Y_n(\eta)=\sum_{k=1}^{N}c_k\sum_{n=1}^{N}\frac{1}{\sqrt{N_n}}v_{nk}^+\,e^{-\mu_k\xi}\,Y_n(\eta), \quad 0<\eta<1 \tag{42}$$

$$\theta(\xi,\eta,\tau)=e^{i\Omega\tau}\sum_{k=1}^{N}c_k\sum_{n=1}^{N}\frac{1}{\sqrt{N_n}}v_{nk}^+\,e^{-\mu_k\xi}\,Y_n(\eta), \quad 0<\eta<1. \tag{43}$$

At the centerline of the duct ($\eta=0$), equation (42) could be written as

$$\theta(\xi,0,\tau)=e^{i\Omega\tau}\sum_{k=1}^{N}c_k\sum_{n=1}^{N}\frac{1}{\sqrt{N_n}}v_{nk}^+Y_n(0)\,e^{-\mu_k\xi}=e^{i\Omega\tau}\sum_{k=1}^{N}c_kg_k\,e^{-\mu_k\xi}=e^{i\Omega\tau}\sum_{k=1}^{N}G_k\,e^{-\mu_k\xi} \tag{44}$$

where

$$g_k = \sum_{n=1}^{N} \frac{1}{\sqrt{N_n}} v_{nk}^{+} Y_n(0) \tag{45a}$$

$$G_k = c_k g_k \tag{45b}$$

Lowest order solution

From a simple inspection of the coefficients matrix, we observed that, specifically for smaller values of the dimensionless frequency, Ω, ($\Omega \leqslant 0.5$) [5] and values of the heat capacitance ratio, $a^* \geqslant 0.1$, the diagonal elements will be dominant compared to the off-diagonal elements. This fact suggests a way of obtaining a straightforward approximate solution, i.e. the lowest order solution, by taking $n = k$ in the summation of equation (36a). This corresponds to a decoupled system (36), and shall be a reasonably accurate procedure as long as the diagonal elements of the coefficient matrix do not substantially differ from their eigenvalues. The approximate decoupled system to be solved can then be written as

$$\frac{d\tilde{\theta}_n^1}{d\xi} + (\lambda_n^2 + i\Omega A_{nn})\tilde{\theta}_n^1 = 0, \quad \text{for } \xi > 0 \tag{46a}$$

$$\tilde{\theta}_n^1(0) = f_n, \quad n = 1, 2, \ldots \tag{46b}$$

where the superscript 1 indicates the lowest-order approximation of the corresponding variables. Equations (46) have the explicit solution as

$$\tilde{\theta}_n^1(\xi) = f_n e^{-(\lambda_n^2 + i\Omega A_{nn})\xi} \tag{47}$$

or, once the inversion formula is invoked, we obtain

$$\tilde{\theta}^1(\xi, \eta) = \sum_{n=1}^{\infty} \frac{1}{\sqrt{N_n}} f_n e^{-(\lambda_n^2 + i\Omega A_{nn})\xi} Y_n(\eta). \tag{48a}$$

Substituting equation (48a) into equation (20), the dimensionless temperature of the duct is given by

$$\theta(\xi, \eta, \tau) = e^{i\Omega\tau} \sum_{n=1}^{\infty} \frac{1}{\sqrt{N_n}} f_n e^{-(\lambda_n^2 + i\Omega A_{nn})\xi} Y_n(\eta). \tag{48b}$$

At the centerline of the duct, equation (48b) could be written as

$$\theta(\xi, 0, \tau) = e^{i\Omega\tau} \sum_{n=1}^{\infty} F_n e^{-(\lambda_n^2 + i\Omega A_{nn})\xi} \tag{49}$$

where

$$F_n = \frac{1}{\sqrt{N_n}} f_n Y_n(0). \tag{50}$$

After the time dependence is incorporated, both complete and lowest order solutions can be expressed in polar coordinates as

$$\theta(\xi, \eta, \tau) = A(\xi, \eta) e^{i[\Omega\tau + \phi(\xi)]}. \tag{51}$$

The amplitude $A(\xi, \eta)$ and the phase lag $\phi(\xi, \eta)$ are then obtained from the following expressions:

$$A(\xi, \eta) = \{[\mathrm{Re}(\bar{\theta}(\xi, \eta))]^2 + [\mathrm{Im}(\bar{\theta}(\xi, \eta))]^2\}^{1/2} \tag{52a}$$

$$\phi(\xi, \eta) = \tan^{-1}\left[\frac{\mathrm{Im}(\bar{\theta}(\xi, \eta))}{\mathrm{Re}(\bar{\theta}(\xi, \eta))}\right]. \tag{52b}$$

Based on the above analysis, a computer program was constructed to calculate the dimensionless fluid temperatures inside the duct. The complete solution is readily obtained from equation (44), through the use of IMSL subroutines [11], for complex matrix eigenvalue problems and complex linear systems. By equation (49), the approximate lowest solution is also programmed to assess its range of applicability in terms of the new parameters, namely Bi and a^*.

RESULTS AND DISCUSSION

Since the temperature amplitude governs the temperature distribution inside the duct, all results in this section are presented graphically in terms of the dimensionless temperature amplitude.

In Figs. 2 and 3, the effect of Biot number on the amplitude of the centerline temperature along the duct is presented as a function of dimensionless axial distance, $\xi = (x/D_e)(D_e/d)^2/(Re\,Pr)$ for $\Omega = 0.1$ (the inlet frequency is about 0.01–0.02 Hz corresponding to the flowing air with d about 0.5 in.). It is seen

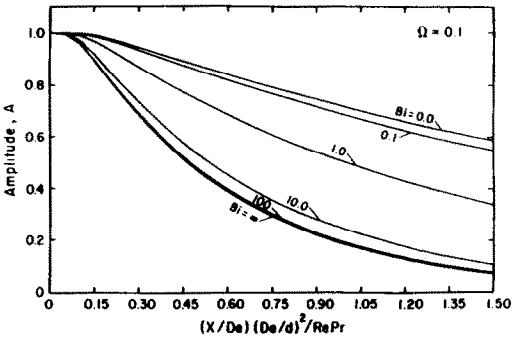

FIG. 2. The effect of Biot number (Bi) on complete solution of dimensionless centerline temperature amplitude for $a^* = 0.1$.

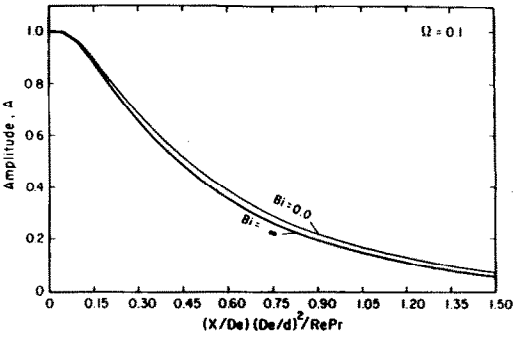

FIG. 3. The effect of Biot number (Bi) on complete solution of dimensionless centerline temperature amplitude for $a^* = 5 \times 10^{-5}$.

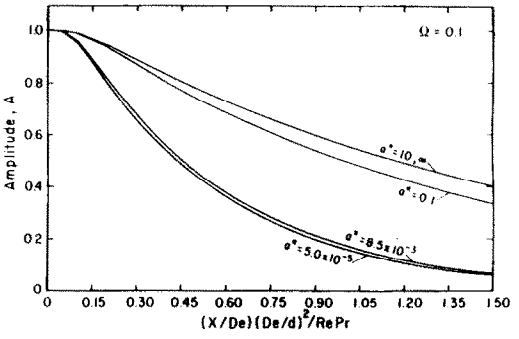

FIG. 4. The effect of fluid-to-wall thermal capacitance ratio (a^*) on complete solution of dimensionless centerline temperature amplitude for $Bi = 1.0$.

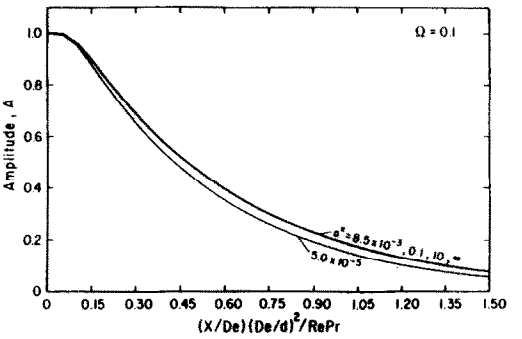

FIG. 6. The effect of fluid-to-wall thermal capacitance ratio (a^*) on complete solution of dimensionless centerline temperature amplitude for $Bi = 100$.

that for the values of $a^* > 0.1$, the effect of Bi on dimensionless temperature amplitude variation is very strong; while for values of $a^* < 5 \times 10^{-5}$, all the temperature amplitude curves along the duct for various values of modified Biot number almost converge (see Fig. 3). For the case of $a^* > 0.1$, the wall thermal capacitance is almost the same order as the thermal capacitance of the fluid; therefore, the dimensionless temperature amplitude is more sensitive to the external convection. For the case of $a^* < 0.1$, the wall thermal capacitance becomes more and more dominant, the heat transferred by the external convection is relatively unimportant compared with the heat storage within the wall, i.e. the influence of Bi on the centerline temperature amplitude along the duct is not significant.

Figures 4–6 illustrate the effects of fluid-to-wall thermal capacitance ratio on the centerline temperature amplitudes along the duct for $Bi = 0.1$, 10 and 100 at $\Omega = 0.1$. It can be seen that for large values of wall thermal capacitance (small $a^* \approx 0.01$), the storage of heat in the wall will substantially affect the dimensionless temperature amplitude along the duct; especially for values of modified Biot number less than 1, which is more important (see Fig. 4). From these three figures, it is clear that the differences among the temperature amplitudes along the duct for different a^* at small values of Bi ($\leqslant 1.0$) are substantial, while those differences for large values of Bi ($\geqslant 10$) are very small, i.e. all the curves for different a^* are very close to each other (see Figs. 5 and 6). When Bi is relatively large ($Bi \geqslant 10$), the heat transfer by external convection is predominant, and the effect of a^* on the temperature amplitude along the duct is either small (for $Bi \approx 10$) or negligible (for $Bi > 10$). For the special case of $Bi = \infty$, all curves for different a^* (from 5×10^{-5} to ∞) will converge to a single curve.

In Fig. 7, the complete solutions with and without considering the effect of the wall thermal capacitance for $Bi = 0.0$ (insulating condition) are compared. It is shown that the temperature amplitude under insulating condition without considering wall thermal capacitance is different from that with considering wall thermal capacitance. With insulation, i.e. with no heat losses, the amplitude should be a constant if the wall thermal capacitance is not taken into account. However, if we consider the wall capacitance, the amplitude is no longer a constant; it decays along the duct even though there is no external convection. This phenomenon should be noted in unsteady heat transfer problems when the thermal capacitance of insulation material to the thermal capacitance of the fluid is very large ($a^* < 0.01$).

In Figs. 8–10, the dimensionless temperature amplitudes along the duct calculated by complete solution and lowest order solution methods are compared. It

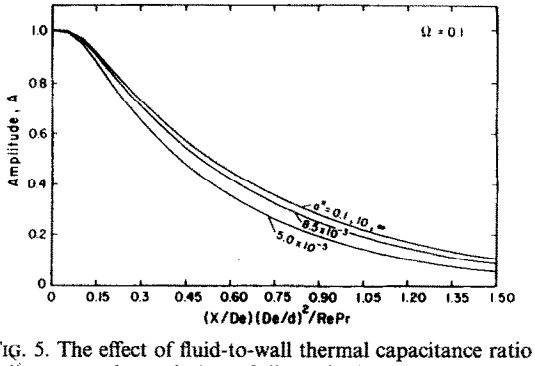

FIG. 5. The effect of fluid-to-wall thermal capacitance ratio (a^*) on complete solution of dimensionless centerline temperature amplitude for $Bi = 10.0$.

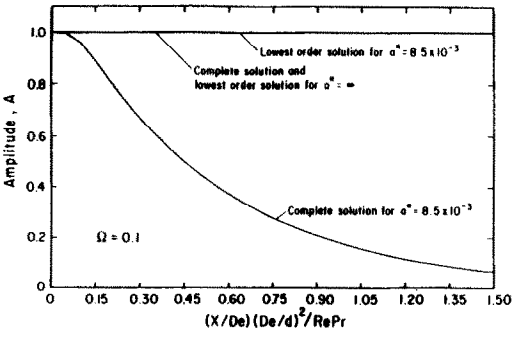

FIG. 7. The comparison of complete solution and lowest order solution of dimensionless centerline temperature amplitude with and without considering the wall thermal capacitance ($a^* = 8.5 \times 10^{-5}$) and for $Bi = 0.0$.

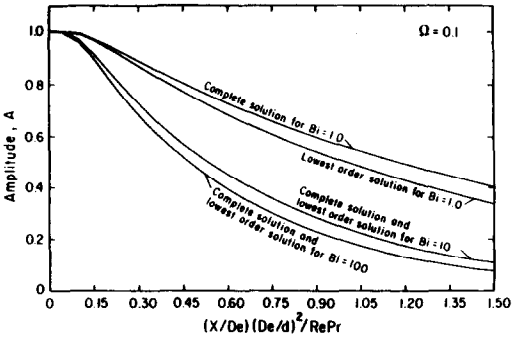

FIG. 8. The comparison of complete solution and lowest order solution of dimensionless centerline temperature amplitude for $a^* = 0.1$ and different Bi (1.0, 10.0, 100).

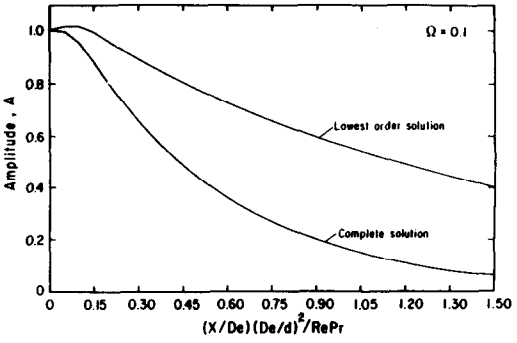

FIG. 10. The comparison of complete solution and lowest order solution of dimensionless centerline temperature amplitude for small Bi ($= 1.0$) and small a^* ($= 5.0 \times 10^{-5}$).

can be seen from these figures that, for the conditions of $a^* > 0.1$ and $Bi \geqslant 10$, complete solution and lowest order solution are identical. For $a^* = 0.1$ and $Bi = 1.0$, the differences between amplitudes of complete and lowest order solution are 0.059 (11.9%) at $\xi = 1.0$ and 0.065 (19.5%) at $\xi = 1.5$ (see Fig. 8). In the range of $5 \times 10^{-5} < a^* < 0.1$, the complete solution and lowest order solution are close to each other. The maximum difference between these two solutions is 0.03 (7.7%) at about $\xi = 0.65$ for the condition of $Bi > 10$ and $a^* = 8.5 \times 10^{-3}$ (see Fig. 9). When the external convection gets less effective, i.e. at very small values of Bi (≈ 1.0), the deviation between two solutions becomes more significant for the small value of a^* (see Fig. 10). From these three figures, it can be concluded that if either $a^* > 0.1$ or $Bi > 10$ is satisfied, the complete solutions could be substituted by the lowest order solutions within reasonable accuracy.

The important results of the theoretical analysis are also given in tabular form; the coefficients (G_k and F_k) and eigenvalues (μ_k and λ_k^2) for equations (44) and (49) are tabulated. In Tables 1–3, the first five coefficients (G_k and F_k) and eigenvalues (μ_k and λ_k^2) are listed for $a^* = 5 \times 10^{-5}$, 8.5×10^{-3} and $a^* > 0.1$ in the absence of the external convection condition. From these three tables, it is obvious that the first coefficients (G_k and F_k) are absolutely dominant, especially for the lowest order solution, however, the first eigenvalues are quite different, which is responsible for the decay of the temperature amplitude away from the inlet. Under the conditions of Tables 1–3, the complete solution is recommended since the lowest solution cannot predict the temperature variation inside the duct correctly. In Tables 4–6, the first ten coefficients (G_k and F_k) and eigenvalues (μ_k and λ_k^2) are given for $Bi = 0.1$, 1, $\geqslant 10$ and $a^* = 8.5 \times 10^{-3}$. Tables 7, 6 and 8 give the first ten coefficients (G_k and F_k) and eigenvalues (μ_k and λ_k^2) for $a^* = 5 \times 10^{-5}$, 8.5×10^{-3}, and $\geqslant 0.1$ for the condition of $Bi = 10$. The last three tables could be used for the condition of $Bi \geqslant 10$. By the use of equations (44) and (49) and these tables, the transient temperature response along the channel could be calculated for different boundary conditions. For the cases of $Bi > 10$, the tables of $Bi \geqslant 10$ at the same a^* could be used for substitution. From any table, it is clear that the higher mode of the eigenvalue increases faster. Thus, the effects of those high eigenvalues on the amplitude decrease as eigenvalues increase. Away from the inlet of the duct, only a few of the smaller eigenvalues persist in the calculation while the exponential of high order of eigenvalue approaches zero much faster.

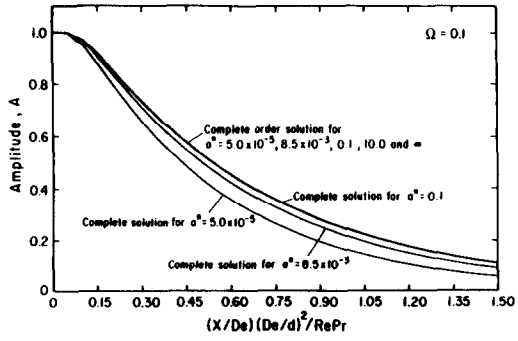

FIG. 9. The comparison of complete solution and lowest order solution of dimensionless centerline temperature amplitude for $Bi = 10.0$ and different a^* (5.0×10^{-5}, 8.5×10^{-3}, 0.1).

CONCLUDING REMARKS

The analytical solutions to the periodic variation of inlet temperature indicate that the fluid temperature amplitude decays exponentially with distance along the duct. At a fixed frequency, the higher order modes tend to zero so fast that ultimately only the basic modes usually remain away from the inlet. This has been demonstrated in the given tables. The eigenvalues and series coefficients for complete solutions and lowest order solutions (see equations (46) and (50)) are very close to each other for $Bi \geqslant 10$ or $a^* \geqslant 0.1$, therefore the complete solutions could be substituted by the lowest order solutions for those conditions.

The effect of external convection, i.e. Biot number, on the temperature responses along the duct is only important in the case of fluid-to-wall thermal capaci-

Table 1. The first five coefficients and eigenvalues of considering the effects of wall capacitance, at $Bi = 0.0$ and $a^* = 5 \times 10^{-5}$ for both complete and lowest order solutions

k	G_k	μ_k	F_k	λ_k^2
1	0.12072E+1+0.82011E−3i	0.20117E+1+0.72862E−1i	0.10007E+1	0.09968E−9
2	−0.31090E+0−0.95008E−3i	0.22407E+2+0.10293E+0i	−0.11940E−7	0.12243E+2
3	0.17008E+0+0.25348E−3i	0.64738E+2+0.13061E+0i	−0.03955E−9	0.45918E+2
4	−0.11588E+0−0.20364E−3i	0.12892E+3+0.16401E+0i	0.21339E−8	0.10090E+3
5	0.86484E−1+0.11591E−3i	0.21494E+3+0.20350E+0i	0.15535E−8	0.17719E+3

Table 2. The first five coefficients and eigenvalues of considering the effects of wall capacitance, at $Bi = 0.0$ and $a^* = 8.5 \times 10^{-3}$ for both complete and lowest order solutions

k	G_k	μ_k	F_k	λ_k^2
1	0.12093E+1+0.14771E−1i	0.19728E+1+0.37485E+0i	0.10007E+1	0.09967E−9
2	−0.31598E+0−0.27488E−1i	0.22009E+2+0.24615E+1i	−0.11940E−7	0.12243E+2
3	0.17698E+0+0.23946E−1i	0.63521E+2+0.61060E+1i	−0.03955E−9	0.45918E+2
4	−0.12470E+0−0.22536E−1i	0.12632E+3+0.11277E+2i	0.21339E−8	0.10090E+3
5	0.97274E−1+0.21628E−1i	0.21027E+3+0.18089E+2i	0.15535E−8	0.17719E+3

Table 3. The first five coefficients and eigenvalues of considering the effects of wall capacitance, at $Bi = 0.0$ and $a^* = 0.1$ for both complete and lowest order solutions

k	G_k	μ_k	F_k	λ_k^2
1	0.10648E+1+0.11674E+0i	0.40422E+0+0.92886E+0i	0.10007E+1	0.09968E−9
2	−0.72035E−1−0.15280E+0i	0.12772E+2+0.28317E+1i	−0.11940E−7	0.12243E+2
3	0.99273E−2+0.52130E−1i	0.46262E+2+0.35029E+1i	−0.03955E−9	0.45918E+2
4	−0.28407E−2−0.25643E−1i	0.10116E+3+0.39569E+1i	0.21339E−8	0.10090E+3
5	0.11529E−2+0.15288E−1i	0.17739E+3+0.43358E+1i	0.15535E−8	0.17719E+3

Table 4. The first ten coefficients and eigenvalues for the condition of $Bi = 0.1$ and $a^* = 8.5 \times 10^{-3}$ for both complete solution and lowest order solution

k	G_k	μ_k	F_k	λ_k^2
1	0.12083E+1+0.14892E−1i	0.19703E+1+0.37647E+0i	0.10132E+1	0.95334E−1
2	−0.31556E+0−0.27771E−1i	0.21986E+2+0.24723E+1i	−0.16720E−1	0.12510E+2
3	0.17668E+0+0.24262E−1i	0.63457E+2+0.61296E+1i	0.50738E−2	0.46248E+2
4	−0.12442E+0−0.22911E−1i	0.12619E+3+0.11314E+2i	−0.24796E−2	0.10128E+3
5	0.96982E−1+0.22067E−1i	0.21004E+3+0.18137E+2i	0.14849E−2	0.17760E+3
6	−0.82122E−1−0.23040E−1i	0.31477E+3+0.26820E+2i	−0.99599E−3	0.27521E+3
7	0.71989E−1+0.24388E−1i	0.44003E+3+0.37742E+2i	0.71820E−3	0.39410E+3
8	−0.66679E−1−0.28877E−1i	0.58508E+3+0.51464E+2i	−0.54459E−3	0.53426E+3
9	0.61236E−1+0.34747E−1i	0.74830E+3+0.68634E+2i	0.42851E−3	0.69569E+3
10	−0.53908E−1−0.47135E−1i	0.92611E+3+0.88759E+2i	−0.34686E−3	0.87839E+3

Table 5. The first ten coefficients and eigenvalues for the condition of $Bi = 1.0$ and $a^* = 8.5 \times 10^{-3}$ for both complete solution and lowest order solution

k	G_k	μ_k	F_k	λ_k^2
1	0.12073E+1+0.16102E−1i	0.19432E+1+0.38806E+0i	0.10883E+1	0.66666E+0
2	−0.31352E+0−0.30440E−1i	0.21762E+2+0.25467E+1i	−0.11655E+0	0.14446E+2
3	0.17464E+0+0.27153E−1i	0.62848E+2+0.62744E+1i	0.41902E−1	0.48835E+2
4	−0.12207E+0−0.26247E−1i	0.12497E+3+0.11495E+2i	−0.21721E−1	0.10433E+3
5	0.94131E−1+0.25805E−1i	0.20791E+3+0.18254E+2i	0.13401E−1	0.18102E+3
6	−0.78128E−1−0.27413E−1i	0.31132E+3+0.26646E+2i	−0.91528E−2	0.27894E+3
7	0.66383E−1+0.29108E−1i	0.43470E+3+0.36767E+2i	0.66810E−2	0.39811E+3
8	−0.57822E−1−0.33391E−1i	0.57726E+3+0.48554E+2i	−0.51110E−2	0.53852E+3
9	0.48707E−1+0.36773E−1i	0.73790E+3+0.61435E+2i	0.40488E−2	0.70019E+3
10	−0.38362E−1−0.41609E−1i	0.91572E+3+0.73787E+2i	−0.32948E−2	0.88311E+3

Table 6. The first ten coefficients and eigenvalues for the condition of $Bi \geqslant 10$ and $a^* = 8.5 \times 10^{-3}$ for both complete solution and lowest order solution

k	G_k	μ_k	F_k	λ_k^2
1	0.11935E+1+0.13486E−1i	0.17378E+1+0.27210E+0i	0.11831E+1	0.16056E+1
2	−0.28560E+0−0.25321E−1i	0.20283E+2+0.15247E+1i	−0.26628E+0	0.19426E+2
3	0.14818E+0+0.21260E−1i	0.59454E+2+0.33933E+1i	0.13272E+0	0.57696E+2
4	−0.95736E−1−0.18980E−1i	0.11934E+3+0.56486E+1i	−0.83202E−1	0.11670E+3
5	0.68499E−1+0.16705E−1i	0.20000E+3+0.81609E+1i	0.58334E−1	0.19659E+3
6	−0.52112E−1−0.15319E−1i	0.30150E+3+0.10830E+2i	−0.43738E−1	0.29746E+3
7	0.41212E−1+0.13778E−1i	0.42387E+3+0.13598E+2i	0.34305E−1	0.41936E+3
8	−0.33512E−1−0.12812E−1i	0.56715E+3+0.16410E+2i	−0.27795E−1	0.56235E+3
9	0.27843E−1+0.11652E−1i	0.73139E+3+0.19237E+2i	0.23081E−1	0.72644E+3
10	−0.23467E−1−0.10933E−1i	0.91661E+3+0.22053E+2i	−0.19542E−1	0.91167E+3

Table 7. The first ten coefficients and eigenvalues for the condition of $Bi \geqslant 10$ and $a^* = 5 \times 10^{-5}$ for both complete solution and lowest order solution

k	G_k	μ_k	F_k	λ_k^2
1	0.12074E+1+0.87908E−3i	0.20380E+1+0.74737E−1i	0.11831E+1	0.16056E+1
2	−0.31278E+0−0.10738E−2i	0.22610E+2+0.11844E+0i	−0.26628E+0	0.19426E+2
3	0.17170E+0+0.35013E−3i	0.65249E+2+0.17043E+0i	0.13272E+0	0.57696E+2
4	−0.11735E+0−0.28163E−3i	0.12987E+3+0.23776E+0i	−0.83202E−1	0.11670E+3
5	0.87729E−1+0.16737E−3i	0.21643E+3+0.32016E+0i	0.58334E−1	0.19659E+3
6	−0.70479E−1−0.13095E−3i	0.32493E+3+0.41685E+0i	−0.43738E−1	0.29746E+3
7	0.57845E−1+0.85620E−4i	0.45536E+3+0.52670E+0i	0.34305E−1	0.41936E+3
8	−0.49723E−1−0.54035E−4i	0.60772E+3+0.64880E+0i	−0.27795E−1	0.56235E+3
9	0.42591E−1+0.26202E−4i	0.78203E+3+0.78204E+0i	0.23081E−1	0.72644E+3
10	−0.38012E−1−0.96991E−6i	0.97830E+3+0.92526E+0i	−0.19542E−1	0.91167E+3

Table 8. The first ten coefficients and eigenvalues for the condition of $Bi = 10$ and $a^* \geqslant 0.1$ for both complete solution and lowest order solution

k	G_k	μ_k	F_k	λ_k^2
1	0.11832E+1+0.28043E−2i	0.16072E+1+0.98530E−1i	0.11831E+1	0.16056E+1
2	−0.26652E+0−0.44836E−2i	0.19435E+2+0.26122E+0i	−0.26628E+0	0.19426E+2
3	0.13289E+0+0.29336E−2i	0.57712E+2+0.46224E+0i	0.13272E+0	0.57696E+2
4	−0.83323E−1−0.23917E−2i	0.11672E+3+0.67820E+0i	−0.83202E−1	0.11670E+3
5	0.58424E−1+0.19280E−2i	0.19662E+3+0.90549E+0i	0.58334E−1	0.19659E+3
6	−0.43807E−1−0.16554E−2i	0.29749E+3+0.11303E+1i	−0.43738E−1	0.29746E+3
7	0.34359E−1+0.14193E−2i	0.41940E+3+0.13573E+1i	0.34305E−1	0.41936E+3
8	−0.27837E−1−0.12514E−2i	0.56238E+3+0.15782E+1i	−0.27795E−1	0.56235E+3
9	0.23116E−1+0.11069E−2i	0.72648E+3+0.17974E+1i	0.23081E−1	0.72644E+3
10	−0.19569E−1−0.99553E−3i	0.91170E+3+0.20122E+1i	−0.19542E−1	0.91167E+3

tance ratio, $a^* > 0.1$. For $a^* < 5 \times 10^{-5}$, all the curves for different external convection are confined to a very small region. For strong external convection ($Bi \geqslant 10$), the effect of thermal capacitance ratio a^* is very small or negligible. As external convection gets less effective ($Bi < 1.0$), the effects of a^* are quite important and cannot be neglected. In the extreme case, $Bi = 0.0$ (insulated boundary condition), the effects of a^* are very large, implying that, in transient forced convection it is necessary to consider the thermal capacitance of the insulating material, which directly affects the thermal responses inside the channel. In heat exchanger equipment, the thermal capacitance of insulating material should be considered for the unsteady operation. Even if there is no external convection in unsteady operation, the boundary condition may not be simply thought of as no heat losses as we did in steady state.

Acknowledgements—The authors wish to thank M. Padki and Dean Brown for their assistance during the preparation of this manuscript. This work was partially supported by NSF through grant No. CBT-860 3997. This paper was revised and finalized during Dr Kakac's stay at the Lehrstuhl A für Thermodynamik, Technische Universität München, as the Recipient of the Senior Scientists Award from the Alexander von Humboldt Stiftung.

REFERENCES

1. E. M. Sparrow and F. N. De Farias, Unsteady heat transfer in ducts with time varying inlet temperature and participating walls, *Int. J. Heat Mass Transfer* **11**, 837 (1968).

2. S. Kakac and Y. Yener, Exact solution of transient forced convection energy equation for timewise variation of inlet temperature, *Int. J. Heat Mass Transfer* **16,** 2205 (1973).
3. S. Kakac, A general analytical solution to the equation of transient forced convection with fully developed flow, *Int. J. Heat Mass Transfer* **18,** 1449 (1975).
4. R. M. Cotta and M. N. Ozisik, Laminar forced convection inside ducts with periodic variation of inlet temperature, *Int. J. Heat Mass Transfer* **29,** 1495 (1986).
5. R. M. Cotta, M. D. Mikhailov and M. N. Ozisik, Transient conjugated forced convection in ducts with periodically varying inlet temperature, *Int. J. Heat Mass Transfer* **30,** 2073 (1987).
6. S. Kakac, Y. Ding and W. Li, Transient fluid flow and heat transfer in ducts with a timewise variation of inlet temperature, *Proc. 3rd Int. Symp. on Transport Phenomena in Thermal Control.* Hemisphere, New York (1989).
7. S. Kakac, Y. Ding and W. Li, Experimental investigation of transient laminar forced convection in ducts, *Proc. Int. Conf. on Experimental Heat Transfer, Fluid Mechanics and Thermodynamics*, Dubrovnik, Yugoslavia, 4–9 September 1988. Elsevier Science, Amsterdam (1989).
8. S. Kakac, W. Li and R. M. Cotta, Theoretical and experimental study of transient laminar forced convection in a duct with timewise variation of inlet temperature, *Proc. ASME Winter Annual Meeting*, San Francisco, California, 15–19 December (1989).
9. S. Kakac, W. Li and R. M. Cotta, Unsteady laminar forced convection in ducts with periodic variation of inlet temperature, *Trans. ASME, J. Heat Transfer* **112,** 913 (1990).
10. M. D. Mikhailov and N. L. Vulchanov, A computational procedure for Sturm–Liouville problems, *J. Comp. Phys.* **50,** 323 (1983).
11. S. Kakac, W. Li and Y. Ding, Transient forced convection in ducts, Interim Report, NSF Project CBT-860 3997 (1988).
12. *IMSL Library*, Edition 7, GNB Building, 7500 Ballaine Blvd., Houston, TX 77036 (1979).

TRANSFERT THERMIQUE VARIABLE DANS UNE ENTREE POUR UN ECOULEMENT LAMINAIRE AVEC VARIATION PERIODIQUE DE LA TEMPERATURE D'ENTREE

Résumé—On présente une étude théorique de la convection laminaire forcée dans la région d'entrée d'un conduit rectangulaire, soumise à une température d'entrée variant sinusoïdalement. On considère plusieurs conditions aux limites qui tiennent compte d'un flux pariétal uniforme et/ou de convections externes avec ou sans effet de capacitance thermique de paroi. Des expressions analytiques sont obtenues à partir de la technique généralisée de la transformée intégrale. Les amplitudes de température sur l'axe sont déterminées en fonction du nombre de Biot, du rapport des capacitances thermiques fluide/paroi et de la fréquence adimentionnelle des oscillations thermiques à l'entrée. On discute les effets de ces paramètres sur la solution. Les valeurs propres et les coefficients correspondants sont donnés sous forme tabulée.

INSTATIONÄRER WÄRMEÜBERGANG IM EINLAUFBEREICH EINER LAMINAREN STRÖMUNG MIT PERIODISCHER ÄNDERUNG DER EINTRITTSTEMPERATUR

Zusammenfassung—Die laminare erzwungene Konvektionsströmung im thermischen Einlaufgebiet eines Rechteckkanals wird untersucht, wobei die Eintrittstemperatur sinusförmig schwankt. Dabei werden verschiedene Randbedingungen betrachtet: gleichförmige Wärmestromdichte an der Wand und/oder äußere Konvektionsströmungen mit oder ohne Einflüsse der Wärmekapazität der Wand. Für diese Probleme werden durch Erweiterung der verallgemeinerten Integral-Transformationstechnik analytische Ausdrücke ermittelt. Die Temperaturamplituden im Strömungskern werden als Funktion der Biot-Zahl, des Verhältnisses der Wärmekapazitäten von Fluid und Wand sowie der dimensionslosen Frequenz der Temperaturschwankung am Eintritt bestimmt. Der Einfluß dieser Variablen auf die Lösung wird diskutiert. Die Eigenwerte und die entsprechenden Koeffizienten werden tabellarisch angegeben.

НЕУСТОЙЧИВЫЙ ТЕПЛОПЕРЕНОС НА ТЕПЛОВОМ ВХОДНОМ УЧАСТКЕ ПРИ ЛАМИНАРНОМ ТЕЧЕНИИ С ПЕРИОДИЧЕСКИМ ИЗМЕНЕНИЕМ ТЕМПЕРАТУРЫ НА ВХОДЕ

Аннотация—Теоретически исследуется ламинарная вынужденная конвекция на тепловом входном участке канала прямоугольного сечения в условиях синусоидального изменения температуры на входе. Рассматриваются несколько видов граничных условий с учетом однородного теплового потока на стенке и (или) внешней конвекции при наличии или отсутствии эффектов теплоемкости стенки. Посредством модификации обобщенного метода интегральных преобразований получены аналитические решения исследуемых задач. Определяются амплитуды температуры на средней линии как функции числа Био, отношения теплоемкостей жидкости и стенки, а также безразмерной частоты тепловых осцилляций на входе. Обсуждается влияние указанных переменных на решение. Приводятся таблицы собственных значений и соответствующих коэффициентов.